VI International Conference on Computational Bioengineering
ICCB 2015
M. Cerrolaza and S.Oller (Eds)

NUMERICAL SIMULATION OF 2D BACTERIAL BIOFILM GROWTH USING THE COMBINED TDG-FIC FINITE ELEMENT METHOD

ICCB 2015

D. FENG[*], I. NEUWEILER[*] AND U. NACKENHORST[†]

[*] Institute of Fluid Mechanics and Environmental Physics in Civil Engineering
Leibniz Universität Hannover
Appelstraße 9a, 30167 Hannover, Germany
e-mail: feng@hydromech.uni-hannover.de, neuweiler@hydromech.uni-hannover.de
www. hydromech.uni-hannover.de

[†] Institute of Mechanics and Computational Mechanics
Leibniz Universität Hannover
Appelstraße 9a, 30167 Hannover, Germany
email: nackenhorst@ibnm.uni-hannover.de, www. ibnm.uni-hannover.de

Key words: biofilm modeling, numerical simulation, time dependent advection-reaction (ADR) equation, finite element, TDG, FIC

Abstract. Bacterial biofilm plays a vital role for many technical and medical applications. Predicting biofilm growth with mathematical models requires solving the balance equations for species and nutrients as well as for biofilm numerically. We consider the model in the continuum mechanics framework, which means the growth of different components of biofilm is governed by a time dependent advection-reaction (AR) equation. To find fast and robust solution schemes for the advection-diffusion-reaction (ADR) equation is challenging, especially under the situation of convection-dominated transport and highly nonlinear reaction terms involved. In this paper, the recently developed time discontinuous Galerkin (TDG) method combined with a stabilization technique called finite calculus (FIC) method has been successfully applied to solve a multi-dimensional multi-species biofilm growth model. The biofilm interface in the model is described as a convective movement following a potential flow coupled to the reaction inside of the biofilm. Nutrients (oxygen in this paper) diffuse through a boundary layer on top of the biofilm interface. A rolling ball method is applied to obtain a boundary layer of constant height. Different patterns of biofilm during the growth obtained from the numerical simulations are studied, and the influence of the parameters on the patterns and the performance of the model are also discussed in this paper.

1 INTRODUCTION

Bacterial biofilms are notorious, especially in clinical applications. They are responsible for most of human infections, and meanwhile the disinfection rate by antibiotic of a biofilm normally is much lower than planktonic bacteria. Even though the definition of biofilm is very diverse, some common components of bacterial biofilms are widely observed form experimental studies, such as the active bacteria, inert or dead bacteria and the extracellular polymeric substance (EPS) produced by the active bacteria. The combination of those

components may influence the profile of biofilms as well as the patterns of biofilms generated.

To predict biofilm growth, numerical models are useful. However various modeling strategies are discussed in literature. Generally, there are two main categories of biofilm models, the continuum models [1] [2] and discrete element based models [3] [4].

Continuum biofilm models differ, depending on the assumptions are made. In this paper, a multi-dimensional multi-species biofilm model developed by Alpkvist and Klapper (A-K model) [1] is used by considering two different components of biomass namely the active biomass and inert biomass within a biofilm. We present a new numerical strategy to simulate the biofilm growth process with the A-K model. The time discontinuous Galerkin (TDG) method [5] is applied to solve the transport equations of biomasses. The instability property that comes from the advection part of the PDEs is sufficiently controlled by Finite Calculus (FIC) method [6]. The biofilm-fluid interface is captured by setting up a threshold value of the total biomass explicitly. Newton-Raphson method is applied to solve the linearized equations. We assume a boundary layer above the biofilm-fluid interface with a constant thickness. The flow in the boundary layer is not captured by the model, but the diffusion of substrates through the boundary layer is taken into account. The boundary layer is modeled explicitly by using a rolling ball algorithm. The growth limiting substrate (oxygen) diffuses into the biofilm from the top of the boundary layer.

In this paper, the A-K model is briefly presented in the second section, and the numerical aspects will be discussed in the third section. Numerical examples and results will be presented in the fourth section.

2 MATHEMATICAL MODEL

The biofilm model is considered within a computational domain of $\Omega :\rightarrow \left\{ \mathbf{x}=\left(x,z \right):0\le x\le W,0\le z\le H \right\}$ as illustrated in Figure 1.

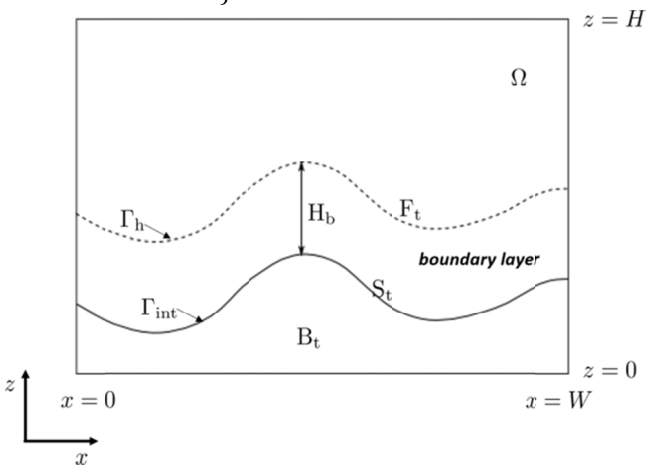

Figure 1: Two-dimensional illustration of the computational domain Ω (Redrawn from [1])

The system contains a time dependent fluid domain F_t and a time dependent biofilm domain B_t, the biofilm-fluid interface is denoted as $\Gamma_{int}=F_t \cap B_t$. The growth of biofilm is limited by the concentration of specific substrates that are known as the growth-limiting substrates. A

boundary layer with a constant thickness is assumed above Γ_{int}. The growth-limiting substrates are assumed to be fully mixed above the boundary layer (the bulk fluid domain) and diffuse from the top of the boundary layer Γ_{h} into the biofilm. The domain below Γ_{h} denotes the time dependent substrates transport domain S_{t}.

The A-K model developed by Alpkvist and Klapper [1] is presented here abbreviatively. Oxygen is chosen as the only biofilm growth-limiting substrate with a concentration of s, and diffuses from the top of the boundary layer Γ_{h}. The mass balance of oxygen reads

$$\begin{aligned} -D\nabla^2 s &= -\upsilon_1 \overline{\rho}\frac{1}{Y}\frac{\mu s}{k_{O_2}+s} && ,\mathbf{x}\in \mathrm{S}_{\text{t}} \\ s &= \overline{s} && ,\mathbf{x}\in \Gamma_{\text{h}} \\ \partial_{\mathbf{n}_s} s &= 0 && ,\mathbf{x}\in \Gamma^s, \end{aligned} \tag{1}$$

where D is the diffusivity of oxygen, and $\overline{s}$ is a constant value of the concentration of oxygen. μ, Y and k_{O_2} are constant parameters of the model and $\overline{\rho}$ is the density of the biofilm. $\Gamma^s :\rightarrow \partial \mathrm{S}_{\text{t}} \cap \partial\Omega$ is the Neumann boundary for oxygen, and $\mathbf{n}_s$ denotes the normal vector of Γ^s. The biofilm growth is modeled as advective transport following a potential flow driven by consumption and production. The biofilm is assumed as a potential flow and thus the growth velocity reads

$$\mathbf{u} = -\lambda \nabla p, \tag{2}$$

where λ is the Darcy constant and $p = p(\mathbf{x},t)$ is the pressure. $\mathbf{x} = \{x, z\}$ refers to the coordinates system of the computational domain. The pressure p is described by

$$\begin{aligned} -\lambda\nabla^2 p &= \upsilon_1\left(\mu\frac{s}{k_{O_2}+s}-\kappa_d\right) && ,\quad \mathbf{x}\in \mathrm{B}_{\text{t}}, \\ p &= 0 && ,\quad \mathbf{x}\in \Gamma_{\text{int}}, \\ \partial_{\mathbf{n}_p} p &= 0 && ,\quad \mathbf{x}\in \Gamma^p, \end{aligned} \tag{3}$$

where $\Gamma^p :\rightarrow \partial \mathrm{B}_{\text{t}} \cap \partial\Omega$ is the Neumann boundaries for pressure. $\mathbf{n}_p$ denotes the normal vectors of Γ^p. Two kinds of biomasses, namely the active biomass and inert biomass, are considered in this paper. The active biomass will grow by consuming oxygen, and it will also decay with a constant rate κ_d. Meanwhile, the active biomass transfers to the inert biomass with an inactivation rate κ_i. Those two kinds of biomasses compose the biofilm. The evolution of the volume fractions of the active biomass υ_1 and the inert biomass υ_2 are described as

$$\begin{aligned} \frac{\partial \upsilon_1}{\partial t} - \lambda\nabla p\cdot\nabla\upsilon_1 &= \upsilon_1\left(\mu\frac{s}{k_{O_2}+s}-\kappa_d-\kappa_i\right)-\upsilon_1^{\,2}\left(\mu\frac{s}{k_{O_2}+s}-\kappa_d\right) && ,\quad \mathbf{x}\in\Omega, \\ \frac{\partial \upsilon_2}{\partial t} - \lambda\nabla p\cdot\nabla\upsilon_2 &= \upsilon_1\kappa_i - \upsilon_1\upsilon_2\left(\mu\frac{s}{k_{O_2}+s}-\kappa_d\right) && ,\quad \mathbf{x}\in\Omega, \\ \partial_{\mathbf{n}_b}\upsilon_j &= 0 \qquad (j=1,2) && ,\quad \mathbf{x}\in\partial\Omega. \end{aligned} \tag{4}$$

where $\mathbf{n}_b$ denotes the normal vectors of $\partial\Omega$.

3 NUMERICAL ASPECTS

In this section, the numerical techniques used in this paper to solve the model described above are presented. Standard Finite Element (Galerkin) method are employed to solve the equations (1) and (3). A combined FIC-TDG method [5] is applied to solve the equations (4). The biofilm-fluid interface is characterized explicitly by a threshold value of total biomass υ^*. A roller ball algorithm is developed to determine the boundary layer of oxygen.

3.1 Time-discontinuous Galerkin (TDG) scheme for advection-reaction PDE

The first publication on TDG method presented by Hughes and Hulbert indicate that the method is A-stable [7]. Recently, Sapotnick and Nackenhorst [5] present a stabilized TDG scheme to solve a group of time dependent advection-diffusion-reaction equations with a combined TDG -FIC method.

The nonlinear time dependent advection-reaction equations (4) can be generally written as

$$\frac{\partial \boldsymbol{\upsilon}}{\partial t} + \mathbf{u}\cdot\nabla\boldsymbol{\upsilon} - f(\boldsymbol{\upsilon}) = 0, \tag{5}$$

where $\boldsymbol{\upsilon} = (\upsilon_1, \upsilon_2)$ is a vector of the volumetric fractions of biomasses. The temporal weak form of equation (5) reads

$$\int_{\mathcal{T}_n} \nu \left(\frac{\partial \hat{\boldsymbol{\upsilon}}}{\partial t} + \mathbf{u}\cdot\nabla\hat{\boldsymbol{\upsilon}} - f(\hat{\boldsymbol{\upsilon}}) \right) \mathrm{d}t = 0, \tag{6}$$

where ν is the weight function in $\mathcal{T}_n =]t_{n-1}, t_n[$ (as shown in Figure 2) which refers to the nth time interval, and $\hat{\boldsymbol{\upsilon}}$ refers to the approximation of the dependent variables in time.

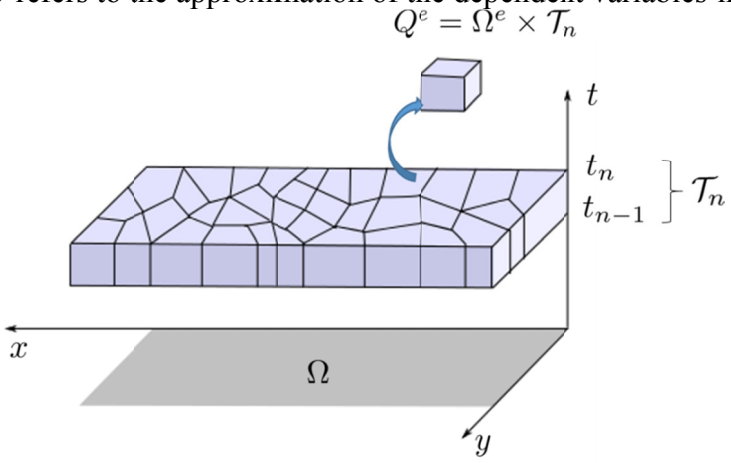

Figure 2: TDG time-space element (Redrawn from [7])

The weight function and the variable value on a discrete node are discontinuous (as shown in Figure 3) in TDG scheme, and the two different values on the same node are marked with "$-$" and "$+$" separately. Integration of equation (6) by part twice yields

$$\int_{\mathcal{T}_n} \nu \left(\frac{\partial \hat{\boldsymbol{\upsilon}}}{\partial t} + \mathbf{u} \cdot \nabla \hat{\boldsymbol{\upsilon}} - f\left(\hat{\boldsymbol{\upsilon}}\right) \right) \mathrm{d}t + \nu_{n-1}^{+} \left[\!\left[\hat{\boldsymbol{\upsilon}}_{n-1} \right]\!\right] = 0, \tag{7}$$

where

$$\left[\!\left[\hat{\boldsymbol{\upsilon}}_{n-1} \right]\!\right] = \hat{\boldsymbol{\upsilon}}_{n-1}^{+} - \hat{\boldsymbol{\upsilon}}_{n-1}^{-}, \tag{8}$$

refers to the jump of $\hat{\boldsymbol{\upsilon}}$ on the discontinuous temporal point t_{n-1},. Discretization of equation (7) in space with standard Finite Element method, the linearized equation (7) is solved iteratively using Newton-Raphson method. The fully discretized equation reads

$$\begin{aligned} &\left[\mathbf{T}_{\mathbf{a}} \otimes \left(\mathbf{N}^T, \mathbf{N} \right)^e + \mathbf{T}_{\mathbf{b}} \otimes \left(\left(-\mathbf{N}_{,\mathbf{x}}^T \mathbf{u}, \mathbf{N} \right)^e - \left(\mathbf{N}^T f'\left(\boldsymbol{\upsilon}_k^h \right), \mathbf{N} \right)^e \right) \right] \Delta \boldsymbol{\upsilon}_k^h \\ &= \mathbf{T}_{\mathbf{c}} \otimes \left(\boldsymbol{\upsilon}_{n-1}^{h-}, \mathbf{N}^T \right)^e - \mathbf{T}_{\mathbf{a}} \otimes \left(\mathbf{N}^T, \mathbf{N} \right)^e \boldsymbol{\upsilon}_k^h \\ &- \mathbf{T}_{\mathbf{b}} \otimes \left[- \left(-\mathbf{N}_{,\mathbf{x}}^T \mathbf{u}, \mathbf{N} \right)^e \boldsymbol{\upsilon}_k^h - \left(f\left(\boldsymbol{\upsilon}_k^h \right), \mathbf{N}^T \right)^e \right], \end{aligned} \tag{9}$$

where

$$\begin{aligned} \left(m, n \right)^e &= \int_{\Omega^e} mn \mathrm{d}\Omega, \\ \mathbf{T}_{\mathbf{a}} &= \int_{\mathcal{T}_n} \widehat{\mathbf{N}}^T \widehat{\mathbf{N}}_{,t} \mathrm{d}t + \widehat{\mathbf{N}}^{+T}\left(t_{n-1} \right) \widehat{\mathbf{N}}^{+}\left(t_{n-1} \right), \\ \mathbf{T}_{\mathbf{b}} &= \int_{\mathcal{T}_n} \widehat{\mathbf{N}}^T \widehat{\mathbf{N}} \mathrm{d}t, \\ \mathbf{T}_{\mathbf{c}} &= \widehat{\mathbf{N}}^{+T}\left(t_{n-1} \right) \widehat{\mathbf{N}}^{-}\left(t_{n-1} \right). \end{aligned} \tag{10}$$

$f'\left(\boldsymbol{\upsilon}_k^h \right)$ denotes the derivate of function $f\left(\boldsymbol{\upsilon}_k^h \right)$, and $\boldsymbol{\upsilon}_k^h$ is the temporal-spatial solution of the independent variables of the k th iteration. $\mathbf{T}_{\mathbf{a}}$, $\mathbf{T}_{\mathbf{b}}$ and $\mathbf{T}_{\mathbf{c}}$ are matrixes only related with the temporal shape functions $\widehat{\boldsymbol{N}}$, and $\boldsymbol{N}$ are the shape functions for spatial approximations.

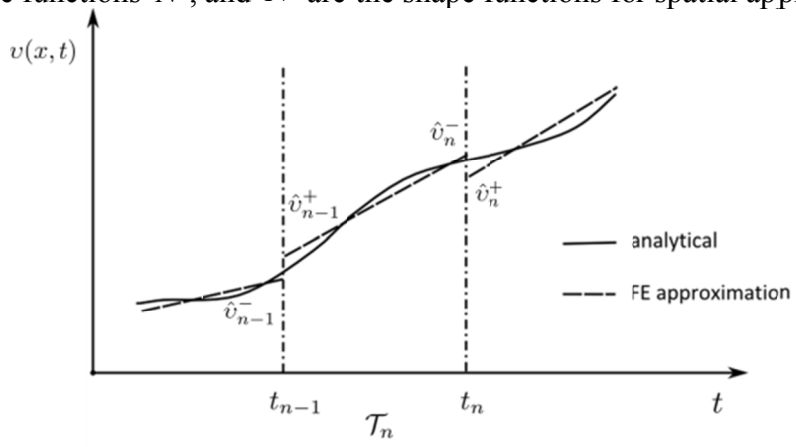

Figure 3: Temporal approximation with linear shape function in TDG scheme (Redrawn from [5])

3.2 Finite calculus (FIC) method for stabilization

The Finite calculus (FIC) method has been firstly introduced by Oñate et al. [6] to stabilize the hyperbolic dominated advection-diffusion-reaction (ADR) PDEs. The basic idea of the FIC method is by considering the balance of flux of a one dimensional problem in a finite domain using Taylor series expansion theory.

Applying the FIC method to the linearized stationary one dimensional advection-reaction equation reads

$$r - \frac{h}{2}\frac{\mathrm{d}r}{dx} = 0, \tag{11}$$

$$r := -u\frac{\mathrm{d}\upsilon}{\mathrm{d}x} + \kappa\upsilon, \tag{12}$$

where h is a characteristic length scale related to the size of the finite domain which differs with different elements, and κ is a reaction coefficient. The FIC formulation of the one dimensional time dependent advection-reaction equation reads

$$\frac{\partial\upsilon}{\partial t} - r + \frac{h}{2}\frac{\mathrm{d}r}{\mathrm{d}x} = 0. \tag{13}$$

Integration of equation (13) with the weight function w leads to the weak form

$$\int_{\Omega}\left(w\upsilon_{,t} + wu\frac{d\upsilon}{dx} - w\kappa\upsilon\right)\mathrm{d}\Omega + \sum_{e}\int_{\Omega_e}\frac{h}{2}w\frac{\mathrm{d}r}{\mathrm{d}x}\mathrm{d}\Omega_e = 0. \tag{14}$$

The last term in equation (14) acts as an additional diffusive contribution to the standard Galerkin procedure as

$$\begin{aligned}
&\sum_{e}\int_{\Omega_e}\frac{h}{2}w\frac{\mathrm{d}r}{\mathrm{d}x}\mathrm{d}\Omega_e \qquad (15)\\
&= -\sum_{e}\int_{\Omega_e}\frac{h}{2}r\frac{\mathrm{d}w}{\mathrm{d}x}\mathrm{d}\Omega_e = -\sum_{e}\int_{\Omega_e}\frac{h}{2}\left(-u\frac{\mathrm{d}\upsilon}{\mathrm{d}x} + \kappa\upsilon\right)\frac{\mathrm{d}w}{\mathrm{d}x}\mathrm{d}\Omega_e\\
&= \sum_{e}\int_{\Omega_e}\frac{h}{2}\left(u - \kappa\upsilon\left(\frac{\mathrm{d}\upsilon}{\mathrm{d}x}\right)^{-1}\right)\frac{\mathrm{d}\upsilon}{\mathrm{d}x}\frac{\mathrm{d}w}{\mathrm{d}x}\mathrm{d}\Omega_e.
\end{aligned}$$

For a two-dimensional case, the additional diffusive contribution is added by transforming the additional element diffusion matrix $\mathbf{D}_e^{curv}$ from the local principle curvature directions (ξ and η) of the solution into the global coordinates [6]

$$\mathbf{D}_e^{FIC} = \mathbf{T}^T\mathbf{D}_e^{curv}\mathbf{T}, \tag{16}$$

where

$$\mathbf{T} = \begin{pmatrix}\cos\varphi & \sin\varphi\\ -\sin\varphi & \cos\varphi\end{pmatrix}, \tag{17}$$

and φ is the angle between the direction of the global coordinate system and the principle curvature direction of the solution.

3.3 Interface and boundary layer

The biofilm-fluid interface is determined by the contour line of the total biomass volume fraction of a constant value υ^*

$$\Gamma_{\text{int}} :\rightarrow \text{contour}\left\{\sum_i \upsilon_i = \upsilon^*\right\}, \tag{18}$$

and $\upsilon^* = 0.9$ is taken in this paper.

A rolling ball algorithm is applied to the contour line Γ_{int} to determine the location of the boundary layer (as illustrated in Figure 4).

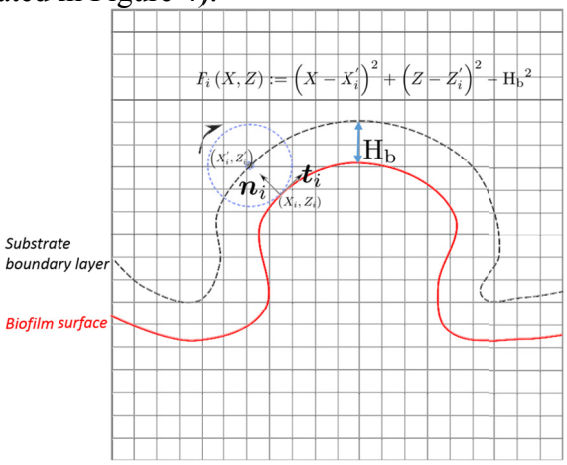

Figure 4: Rolling ball method to determine the boundary layer

The boundary layer is determined by rolling a rigid ball of a radius of $\mathbf{H}_{\text{b}}$ on Γ_{int}, and the trace of the ball's center denotes to Γ_{h}. The detail procedures of the algorithm is illustrated as

1) Compute the tangent vector $\boldsymbol{t}_i$ and normal vector $\boldsymbol{n}_i$ at the point i on $\boldsymbol{\Gamma}_{\text{int}}$
2) Compute the corresponding coordinates $\boldsymbol{X}_i'$ on Γ_{h}

$$\boldsymbol{X}_i' = \boldsymbol{X}_i + \mathrm{H}_{\text{b}}\boldsymbol{n}_i, \tag{19}$$

where $\boldsymbol{X} = (X, Z)$ refers to the coordinates of the biofilm-fluid interface.

3) Check if the ball and the biofilm-fluid interface Γ_{int} overlaps. A distance function is defined as

$$F_i(\boldsymbol{X}) := (X - X_i')^2 + (Z - Z_i')^2 - \mathrm{H}_{\text{b}}^2. \tag{20}$$

For arbitrary point i on Γ_{int}, if $F_i(\boldsymbol{X}) \geq 0$ is always satisfied, point X_i' is marked as a point on Γ_{h}, otherwise, it is not taken as a point on Γ_{h}. An alternative form of $F_i(\boldsymbol{X})$ which can tolerate a certain amount of discrete error is used in this paper as

$$F_i(\boldsymbol{X}) := (X - X_i')^2 + (Z - Z_i')^2 - (\mathrm{H}_{\text{b}} - \delta_i)^2, \tag{21}$$

where δ_i is a parameter that related to the grid size. Here we choose

$$\delta_i = \frac{1}{4}\min\{d_j\}, \qquad \text{for} \quad j = 1,2,...,4 \tag{22}$$

where d_j refers to the length of the edges of the element which contains point i (on Γ_{int}).

4 RESULTS

For computational convenience, the dimensionless form of the governing equations are solved in a dimensionless domain $\Omega_{\text{d}} :\rightarrow [0,1]\times[0,1]$. The dimensionless variables as well as the constant parameters of the model refer to [1]. The initial conditions of the volume fraction of biomasses are given as $\upsilon_1^0 = 1$ and $\upsilon_2^0 = 0$, and the initial biofilm-fluid interface is defined as

$$\Gamma_{\text{int}}^0 :\rightarrow Z = 0.2 + 0.05\sin\left(4\pi X + \frac{\pi}{2}\right). \tag{23}$$

The thickness of the boundary layer is chosen as $\text{H}_\text{b} = 0.15$ (as shown in Figure 5).

Here we present two representative sets of simulation results as shown in Figure 6 and Figure 7. The only difference between those two groups of results is the choice of the inactive rate k_i. For the results shown in Figure 6, an inactive rate of $k_i = 1.0\times10^{-6}$ is taken (refers to set 1), while $k_i = 6.0\times10^{-6}$ is used corresponding to the results shown in Figure 7 (refers to set 2). The decay rate of these two sets of simulations is chosen as $k_d = 2.0\times10^{-6}$. The colours in the figures represent the volume fractions of the biomass. The volume fractions of both the active biomass and the inert biomass after 5 days, 15 days and 20 days are presented. The biofilm-fluid interface Γ_{int} is colored by a white curve in the figures.

Different patterns of biofilm are reproduced by the numerical simulation. The well-known finger pattern is reproduced in set 1, and the flat pattern is observed in set 2. Both of those two sets of simulations show that the active biomass prefer to distribute at the top of the biofilm while the inert one distributes more at the bottom with increasing time. This is due to the growth limiting substrate, which is oxygen in this paper that has a higher concentration at the top of biofilm, and the active biomass is produced by consuming oxygen.

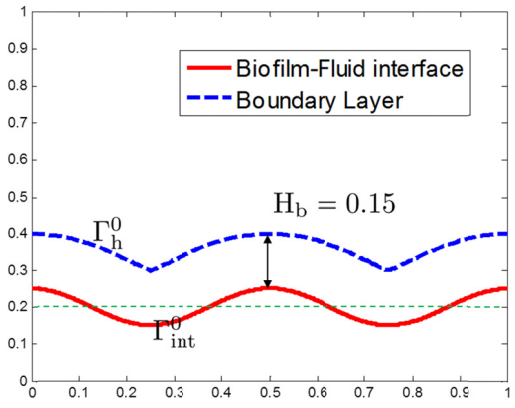

Figure 5: Initial conditions for the biofilm simulation

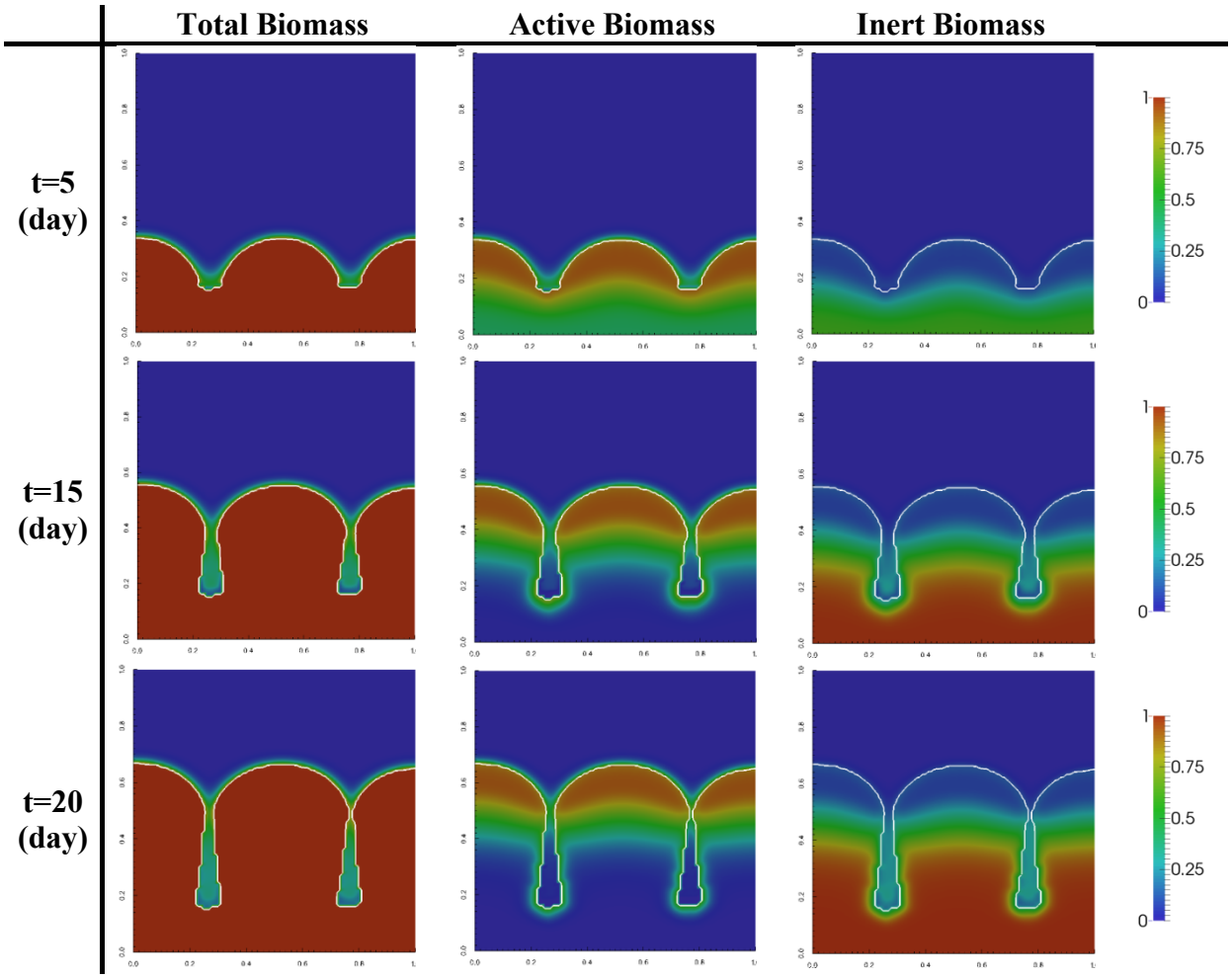

Figure 6: The simulation result of set1 ($k_i = 1.0 \times 10^{-6}$)

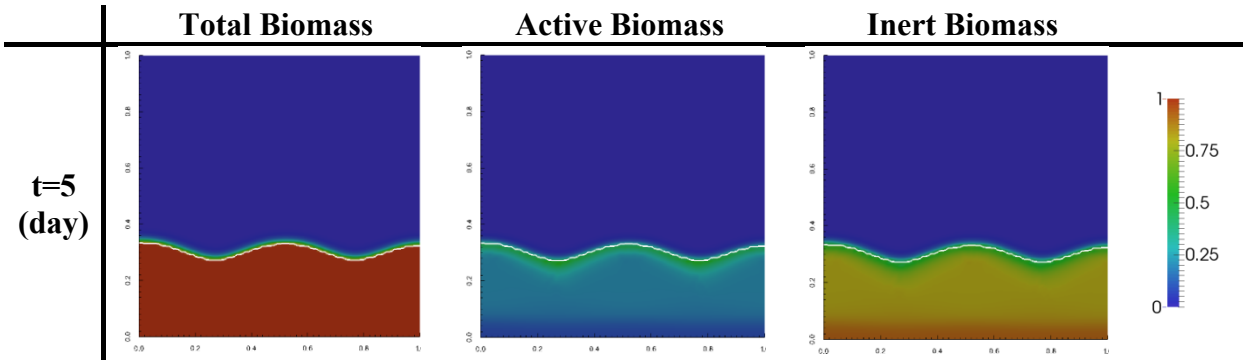

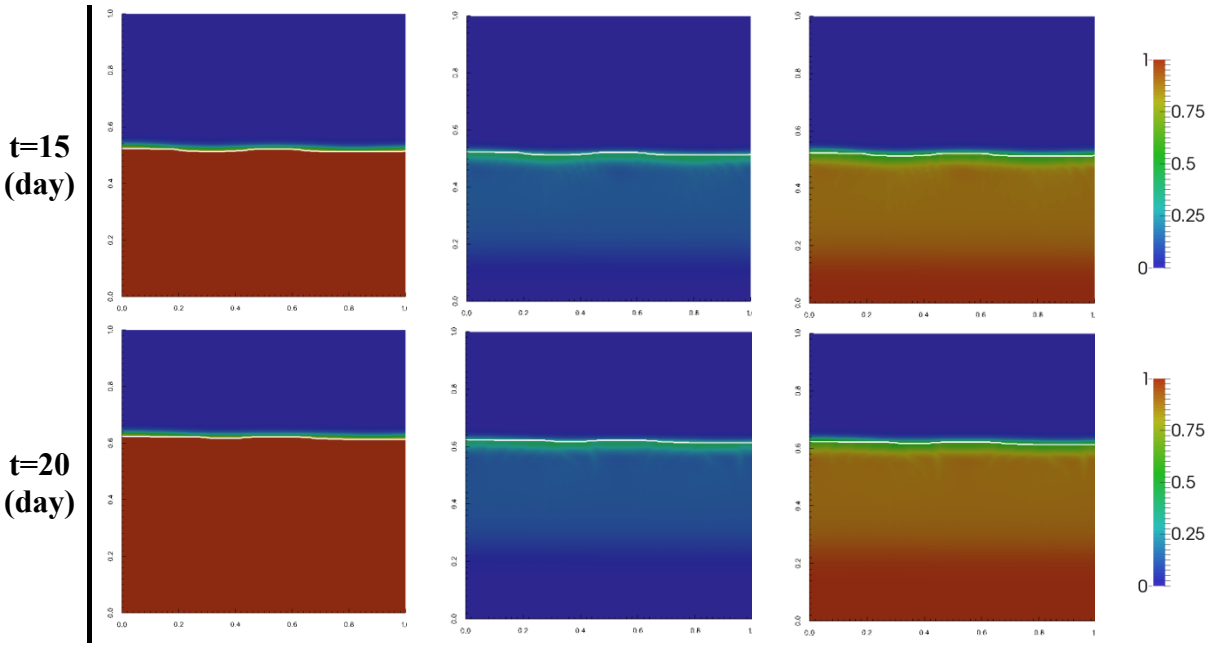

Figure 7: The simulation result of set2 ($k_i = 6.0 \times 10^{-6}$)

5 SUMMARY

A new numerical strategy for simulating biofilm growth with A-K model has been presented in this paper. The combined FIC-TDG finite element method is applied to solve the transport equations of biomasses and a rolling ball algorithm is applied to determine the top of a boundary layer above the biofilm surface.

Different patterns of biofilm are produced by the numerical simulations. The distribution of different biomasses is also observed from the simulation results. The numerical framework presented in this paper is shown to be sufficiently robust to simulate the biofilm growth problem with A-K model.

REFERENCES

[1]Alpkvista, E. and Klapper, I. A Multidimensional Multispecies Continuum Model for Heterogeneous Biofilm Development. *Bull. Math. Biol.* (2007) **69:**765-789.

[2]Eberl, Herman. J, Parker, D. F, and Vanloosdrecht, Mark C. M. A new deterministic spatio-temporal continuum model for biofilm development. *J. Theor. Med.* (2001) **3:**161–175.

[3]Kreft, J.-U, Picioreanu, C, Wimpenny, J. W. T, and van Loosdrecht, Mark CM. Individual-based modelling of biofilms. *Microbiol.* (2001) **147:**2897–2912.

[4]Wimpenny, J. W. T. and Colasanti, R. A unifying hypothesis for the structure of microbial biofilms based on cellular automaton models. *FEMS Microbiol. Ecology* (1997) **22:**1–16.

[5]Sapotnick, A. and Nackenhorst, U. A combined FIC-TDG finite element approach for the numerical solution of coupled advection–diffusion–reaction equations with application to a

bioregulatory model for bone fracture healing. *Int. J. Numer. Meth. Engng* (2012) **92:**301–317.

[6]Oñate, E, Miquel, J, and Zárate, F. Stabilized solution of the multidimensional advection–diffusion–absorption equation using linear finite elements. *Comput. Fluids* (2007) **36:**92–112.

[7]Hughes, T,JR and Hulbert, G. M. Space-time finite element methods for elastodynamics: formulations and error estimates. *Comput. Methood Appl. M.* (1988) **66:**339–363.